

# Volume Transport Variability Southeast of Okinawa Island Estimated from Satellite Altimeter Data

XIAO-HUA ZHU<sup>1\*</sup>, HIROSHI ICHIKAWA<sup>1,2</sup>, KAORU ICHIKAWA<sup>1,3</sup> and KENSUKE TAKEUCHI<sup>1</sup>

<sup>1</sup>Institute of Observational Research for Global Change, Japan Agency for Marine-Earth Science and Technology, Natsushima-cho, Yokosuka 237-0061, Japan

<sup>2</sup>Faculty of Fisheries, Kagoshima University, Shimoarata, Kagoshima 890-0056, Japan

<sup>3</sup>Research Institute for Applied Mechanics, Kyushu University, Kasuga, Fukuoka 816-8580, Japan

(Received 2 September 2003; in revised form 14 January 2004; accepted 26 January 2004)

**A nine-year-long record of the northeastward volume transport (NVT) in the region southeast of Okinawa Island from 1992 to 2001 was estimated by an empirical relation between the volume transport obtained from the ocean mooring data and the sea surface height anomaly difference across the observation line during 270 days from November 2000. The NVT had large variations ranging from  $-10.5$  Sv ( $1$  Sv  $\equiv 10^6$  m<sup>3</sup>s<sup>-1</sup>) to  $30.0$  Sv around its mean of  $4.5$  Sv with a standard deviation of  $5.5$  Sv. This large variation was accompanied by mesoscale eddies from the east, having a pronounced period from 106 to 160 days. After removal of the eddy, NVT was found to fluctuate from 2 Sv to 12 Sv with a quasi-biennial period.**

Keywords:

- Volume transport,
- southeast of Okinawa,
- satellite altimeter,
- long-term monitoring of the volume transport,
- mesoscale eddy.

## 1. Introduction

The Kuroshio transports a large quantity of warm, salty tropical water northward and plays an important role in the global climate system. Estimates of the volume transports of the Kuroshio mainstream in the east of Taiwan (Johns *et al.*, 2001), East China Sea (Ichikawa and Beardsley, 1993) and south of Japan (Imawaki *et al.*, 2001) have been published during the last decade. Compared with the Kuroshio mainstream in the East China Sea, our knowledge of the current in the east of Ryukyu Islands is very poor because only a few mooring observations have been made in this area. Ichikawa *et al.* (2004) detected the stable northeastward current in the southeast of Amami-Oshima Island and suggested that it should exert a great effect on the Kuroshio south of Japan. An understanding of the variation mechanism of the current and monitoring its volume transport in the east of Ryukyu Islands is therefore important for prediction of the Kuroshio mainstream south of Japan.

Lee *et al.* (2001) measured the northward volume transport of the Kuroshio in the east of Taiwan. Comparing their results with the Sverdrup transport at the same latitude, they suggested that the Kuroshio Branch Current may flow in the southeast of Ryukyu Islands. The possibility of a northeastward current over the eastern slope of the southern Ryukyu Islands was first pointed

out by Worthington and Kawai (1972). Yuan *et al.* (1994) and Shiga *et al.* (2000) also showed the possibility of a northeastward current over the continental slope in the southeast of Okinawa Island, on the basis of moored current meter and moored ADCP (acoustic Doppler current profiler) observations, respectively.

The northeastward volume transport in the region southeast of Okinawa was estimated to very widely from 3–10 Sv ( $1$  Sv  $\equiv 10^6$  m<sup>3</sup>s<sup>-1</sup>) by the modified inverse method (Liu and Yuan, 2000). Nakano *et al.* (1998) analyzed the 14 sections of geostrophic current velocity relative to 1500 dbar using hydrographic data from 1987 to 1997, and concluded that no stable northeastward current exists in this area. The above calculations, using the occasional hydrographic data, could not obtain the mean northeastward volume transport, however, because volume transport in the region southeast of Okinawa fluctuates widely due to the mesoscale eddy coming from the east (Zhu *et al.*, 2002).

From November 2000 to August 2001, mooring arrays, including nine inverted echo sounders with pressure gauges (PIESs) and an upward-looking moored ADCP (MADCP), were deployed in the region southeast of Okinawa to examine the current structure and volume transport. A 270-day long time series of geostrophic volume transport was estimated, and the temporal mean volume transport in the upper 2000 dbar layer was estimated to be 6.1 Sv toward the northeast (Zhu *et al.*, 2003). However, since the time interval of the mesoscale eddies entering this area dominated longer than 100 days, the 270-

\* Corresponding author. E-mail: xhzh@jamstec.go.jp

day mean is too short to remove the eddy component. It is also necessary to examine the long period variations of the volume transport, such as seasonal, annual and interannual variations, to study their relationships with the Kuroshio variations and the climate change in the North Pacific.

The current velocity structure in the region southeast of Okinawa changed markedly due to the intrusions of the mesoscale eddies. Yuan *et al.* (1994) first reported a northeastward current with a subsurface northeastward current velocity core, using the modified inverse method in the region southeast of Okinawa, but they could not find a similar northeastward velocity core in February, April and July of 1998 (figures 2(a), (b) and (c) of Liu and Yuan (2000)). In the 14 sections of geostrophic current velocity analyzed by Nakano *et al.* (1998), there was only one section (figure 8(7) of their paper) in which a significant subsurface current velocity core appeared. The 270-day mean geostrophic velocity section estimated from PIES and MADCP data showed a mean barotropic northeastward velocity structure without any subsurface velocity core in the region southeast of Okinawa (Zhu *et al.*, 2003).

In this paper we present a nine-year-long record of the northeastward volume transport (NVT) in the region southeast of Okinawa Island estimated by combined use of the 270-day long volume transport data obtained from ocean mooring data combined with satellite altimeter and tide gauge data. This paper is organized as follows: the data source and data processing are described in Section 2. Estimations of the nine-year-long time series of the NVT by an empirical relation between the NVT obtained from ocean mooring data and sea surface height anomaly difference (SSHAD) across observation line are derived in Section 3. Variabilities of the NVT are shown in Section 4. A discussion and summary are presented in Section 5.

## 2. Data and Data Processing

### 2.1 Volume transport from ocean mooring data

Figure 1 shows the locations of mooring sites of nine PIESs and an MADCP carried out from November 2000 to August 2001. Zhu *et al.* (2003) estimated the volume transport across the line P1–P5 as follows: the specific volume anomaly profiles were derived from the round-trip acoustic travel time by the Gravest Empirical Mode (GEM) method (Watts *et al.*, 2001; Book *et al.*, 2002). Vertical profiles of geostrophic velocity ( $V_G$ ) were calculated from GEM-derived specific volume anomaly profiles. The 270-day-long time series of northeastward geostrophic volume transport across the line P1–P5 was estimated from  $V_G$ . A detailed description of the PIES and MADCP observations and geostrophic calculation is

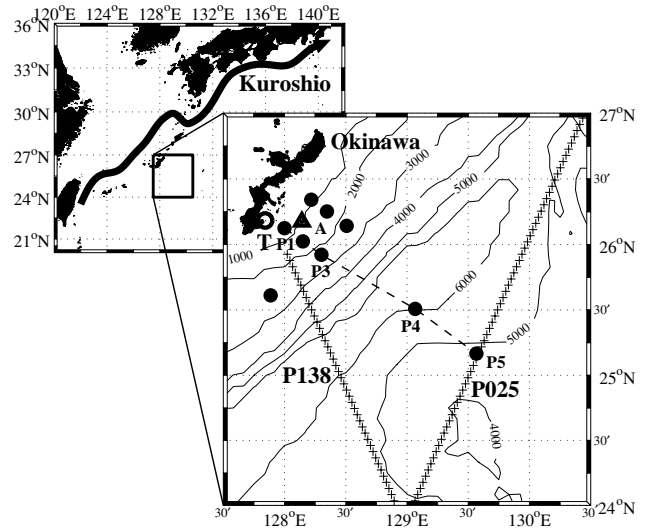


Fig. 1. Location of the observation site. Solid circles (P1, P3, P5 and P9) and open triangle (A) indicate the locations of PIESs and the MADCP, respectively. The open circle (T) southeast of Okinawa Island indicates the tide gauge station. The satellite tracks, Path 025 and Path 138 of the TOPEX/POSEIDON, are indicated with “+”. The broken line from P1 to P5 shows the section where the volume transport was examined. Bathymetric contours are in meters.

given in Zhu *et al.* (2003). This 270-day-long time series of the NVT is used to estimate the nine-year-long record of the NVT only from the time series of the SSHAD.

### 2.2 Satellite altimeter data

There are two satellite tracks (Paths 025 and 138) of the TOPEX/POSEIDON (T/P) altimeter that cross the region southeast of Okinawa (“+” in Fig. 1). Path 025 is the ascending track passing just above the easternmost PIES mooring site of P5. Path 138 is a descending track passing near P1 before the satellite flew over the Okinawa Island. The Sea Surface Height Anomaly (SSHA) data from the nine-year mean of these two T/P tracks were used to compare the mooring data after removal of tide and steric height caused by seasonal warming and cooling in the surface layer. The approaches for removing the steric height in the SSHA are described in detail in Appendix 1.

The T/P altimeter data along the tracks were first passed by a five-point filter (spatial scale about 29 km along the ground track) to decrease the error. Figure 2 shows the spatial pattern of the correlation of the SSHA time series along Path 025 and Path 138 with dynamic height derived from the PIES data. The maximum correlation coefficient of the SSHA for Path 025 (SSHA025) with dynamic height at P5 reached 0.92 (“+” on P025 in

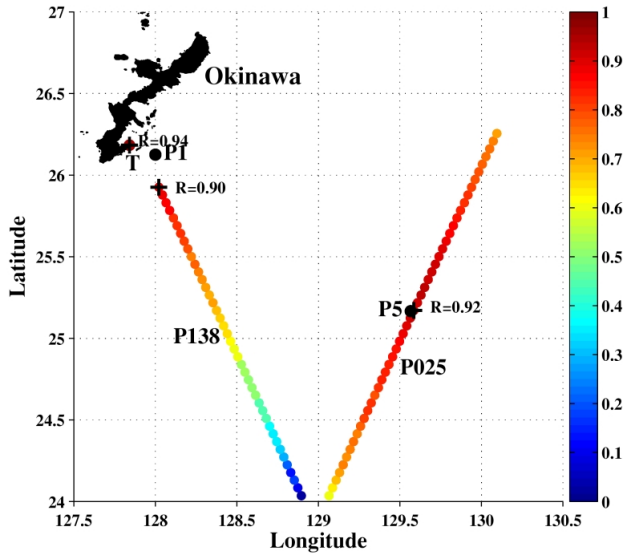


Fig. 2. Spatial pattern of the correlation of TOPEX/POSEIDON time series with the dynamic height derived from PIES data. Color dot lines of P025 and P138 show the correlation coefficient of SSHA along the Path 025 with the dynamic height at P5, and correlation coefficient of the SSHA along the Path 138 with the dynamic height at P1, respectively. The positions of maximum correlation coefficient are indicated with “+”. The correlation coefficient ( $R = 0.94$ ) between sea level of the tide gauge and the dynamic height at P1 is also presented near the tide gauge station.

Fig. 2). There are about 11% missing SSHA data for Path 138 (SSHA138) at the northwest side near Okinawa Island, because altimetry data close to land generally tend to be lost due to a poor ocean tidal model or water vapor corrections. The maximum correlation coefficient of SSHA138 with dynamic height derived from the PIES data at P1 was 0.90.

In addition, in order to identify the relationship between the NVT and mesoscale eddies, the SSHA data derived from the T/P and ERS-1, -2 satellite altimetry data were calculated by optimal interpolation with approximately 150 km and 15 days smoothing scales to obtain the grid data with 0.25 degrees interval every 5 days.

### 2.3 Tide gauge data

The tide gauge station is located 17 km northwest of P1 in the southeast of Okinawa Island (open circle (T) in Fig. 1). Sea level (SL) was measured every hour from 1980 by the Geographical Survey Institute, Ministry of Land, Infrastructure and Transport, Japan. The hourly SL data were first processed by barometric adjustment. The tidal signals were removed by a 48-hour tide killer filter (Hanawa and Mitsudera, 1985), and then the SL data were

applied by a 10-day low pass filter. Finally, the steric height due to the seasonal warming and cooling were removed from the SL data (Appendix 1). The correlation coefficient between the SL and the dynamic height at P1 reached 0.94 (Fig. 2), which suggests that the use of tide gauge data is preferable to the satellite altimeter data in the coastal region. This result is similar to the case in the region south of Shikoku, Japan (Uchida *et al.*, 1998).

## 3. Transport Estimates

### 3.1 Empirical relation between the NVT and the SSHAD

The T/P track and the tide gauge station are very close to both ends of the observational line, across which the volume transport was estimated. A close correlation was found between the dynamic height derived from the PIES data and the SSHA or the SL, which indicates that we can estimate and monitor the NVT across the observational line by the SSHA and the SL data, assuming some relationship exists between the NVT and the surface velocity.

In order to examine the relationships between the NVT in different layers and the SSHAD between the SSHA025 and the SL, we divided the depth layer as follows: (1) the upper seasonal thermocline (0–200 dbar), (2) the permanent (main) thermocline (201–800 dbar), (3) the upper deep layer (801–1200 dbar), to which the effect of eddy can reach (Zhu *et al.*, 2003), (4) the deep layer (1201–2000 dbar), to which the eddy effect cannot reach; in addition, the total layer upper of 2000 dbar is also considered (5). Figures 3(a)–(e) show scatter plots of the 10-day interval volume transports in the different vertical layers and the SSHAD. The correlation coefficient between volume transports in the upper 2000 dbar and the SSHAD is 0.92, and the rms (root-mean-square) difference from the regression line is 2.8 Sv (Fig. 3(e)). The volume transport varies from  $-9.5$  to 20.8 Sv, corresponding to an SSHAD change from  $-36$  to 34 cm. The volume transport of about 8 Sv at the SSHAD = 0 during the 270-day period, indicates that a mean current flows northeastward. The reader should note that the SSHAD = 0 is the mean state (i.e. no eddy) of the observation line.

The correlation coefficients are 0.91 in the upper seasonal thermocline, 0.92 in the permanent thermocline and 0.90 in the upper deep layer, being almost as high as that in the upper 2000 dbar layer. On the other hand, it is 0.53 in the deep layer, which is much smaller than the others. Figure 3 demonstrates that the volume transports in the upper three divided layers are proportional to each other, but not proportional to the deep layer (1201–2000 dbar). The transport and its variance in the deep layer, however, is about 0.5 Sv (Fig. 3(d)), which is only about 1.7% of the total volume transport in the upper of 2000 dbar. The close correlation between the SSHAD and the

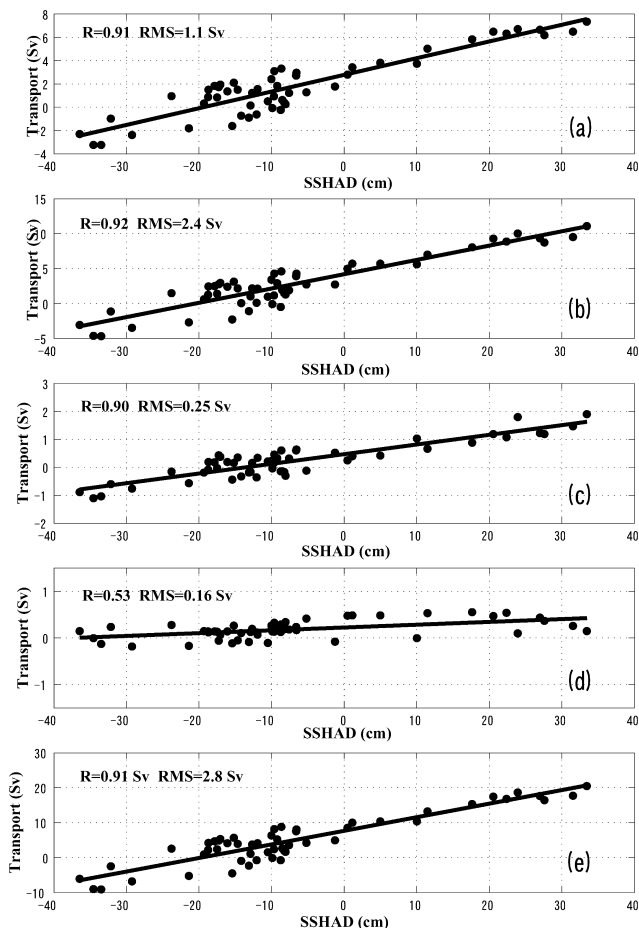


Fig. 3. Scatter plots of the NVT (Sv) in upper 200 dbar (a), 201–800 dbar (b), 801–1200 dbar (c), 1201–2000 dbar (d) and 0–2000 dbar (e) against the sea surface height anomaly difference (SSHAD, unit: cm) across the line P1–P5. The solid line in each panel is the regression line. The correlation coefficient and the root-mean-square difference from the regression line are shown in the upper-left corner of each panel. The SSHAD is the difference between the SSHA near P5 (“+” in Fig. 2) obtained from T/P data and the sea level measured with the tide gauge in the southeast of Okinawa coast.

volume transport in the upper 2000 dbar layer implies that the SSHAD is proportional to the volume transport in the upper 1200 dbar layer, and the very small volume transport in the deep layer has a low correlation with the SSHAD.

These results allowed us to utilize the SSHAD to estimate the volume transport in the upper 2000 dbar. This calculation process is similar to that used for the ASUKA (Affiliated Surveys of the Kuroshio off Cape Ashizuri) line in the region south of Shikoku (Imawaki *et al.*, 2000). These authors examined the normalized transport profiles and found that the Kuroshio transports in upper 1000 dbar

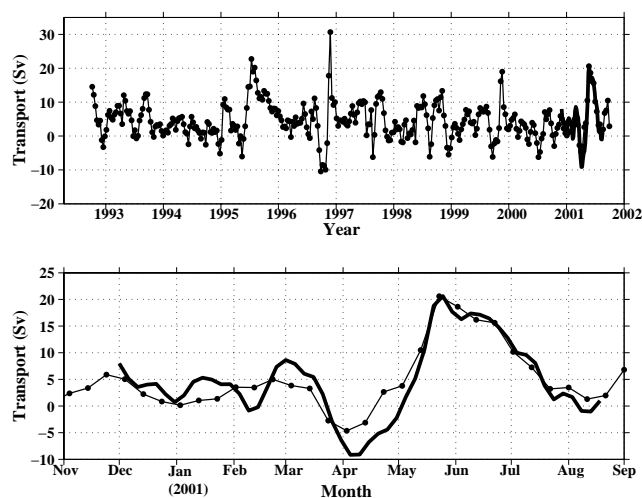


Fig. 4. Time series of the NVT. Thin lines with dots indicate the NVT estimated from TOPEX/POSIDON altimeter data and tide gauge data using the empirical relation between the NVT and the SSHAD across the P1–P5. The solid lines indicate the NVT estimated from ocean mooring data. Upper panel shows the nine-year-long time series of the NVT from 1992 to 2001. Bottom panel shows the magnified time series of the NVT from November 2000 to August 2001 during the ocean mooring period. Tick marks along the bottom of time axes indicate the beginning of a year (month).

are proportional to the surface transports, although our case is much more complex. It is difficult to normalize the transport profiles by the surface transport, because the surface transports change direction, and sometimes become zero.

### 3.2 Estimation of nine-year-long record of the NVT

We now use the correlation between the volume transport and the sea surface height anomaly difference to provide the long-term record of the estimated NVT across the line P1–P5 in the region southeast of Okinawa using the same method as proposed by Imawaki *et al.* (2000). The T/P altimeter data of Path 025 at P5 for first 365 repeat cycles and the corresponding tide gauge data are processed. Figure 4 shows the nine-year-long record of estimated transport from 1992 to 2001 with a 10-day interval.

The estimated transport fluctuates widely from  $-10.5$  to  $30.0$  Sv around a mean of  $4.5$  Sv with a standard deviation of  $\pm 5.5$  Sv. The estimated NVT agrees well with that derived from PIES data, except in April 2002 during the cold eddy period (bottom panel of Fig. 4). Usually, the cold eddy (warm eddy) can raise (reduce) the thermocline, which means the upper layer becomes thin (thick) and the deep layer becomes thick (thin). The ocean observation data also showed the thermocline declined

by about 200 dbar from April to July 2002 during the change from the cold eddy period to warm eddy period (Zhu *et al.*, 2002). Theoretically, the vertical structure of the velocity may be changed during the cold eddy and warm eddy events, so the above empirical equation for converting the SSHAD into the NVT may be different. But the mean NVT per unit depth for cold/warm eddy periods are actually 47.8%/48.6% (for 201–800 dbar) and 14.8%/10.1% (for 801–1200 dbar) of those in the upper 200 dbar layer, respectively, which means the ratio of the NVT between the deep layer and the surface layer is almost the same during the cold and warm eddy periods. We also tried to create another empirical equation using only the data when the SSHAD < 0 for the cold eddy period, but this virtually did not change the inclination of the regression line or the correlation coefficient, which means that the empirical relation for converting the SSHAD into the NVT is almost the same during both cold and warm eddy periods. This may be due to the smoothing and interpolating effects in the GEM method. However, because the rms differences of 2.8 Sv between the SSHAD and the NVT is sufficiently small compared to the ocean observation error of 5.1 Sv (Appendix 2), for simplicity we used the same empirical equation to estimate the NVT from the SSHAD.

Errors of the NVT estimated from the SSHAD include the following three components: 1) error due to the accuracy of the estimated NVT using the PIES data and MADCP data is 5.1 Sv; 2) error due to the T/P altimeter measurement error and tide level measurement error is 0.7 Sv; and 3) error caused by using the regression relationship is 2.8 Sv. These three error components could propagate and generate an error of 5.9 Sv in the final results through the calculations. A detailed description of the error estimation is given in Appendix 2.

#### 4. Variability of the Volume Transport

##### 4.1 Variability due to mesoscale eddies

Figure 5 shows the power spectra of the nine-year record of the NVT. A pronounced peak appears around the period from 106 to 160 days. This variation may be accompanied by the intrusion of anticyclonic and cyclonic eddies into the region. A roughly 100-day period variation of velocity and northeastward volume transports in the southeast Okinawa Island was found by Zhu *et al.* (2002), but they could not identify the accurate period, because they only had available 270-day long time series of the velocity and the NVT. The 100-day period variations were also found in the northeast of Taiwan (the southernmost of Ryukyu Islands) due to eddies coming from the east (Yang *et al.*, 1999).

From 1992 to 2001, the NVT experienced the greatest changes four times: from April to July 1995, Septem-

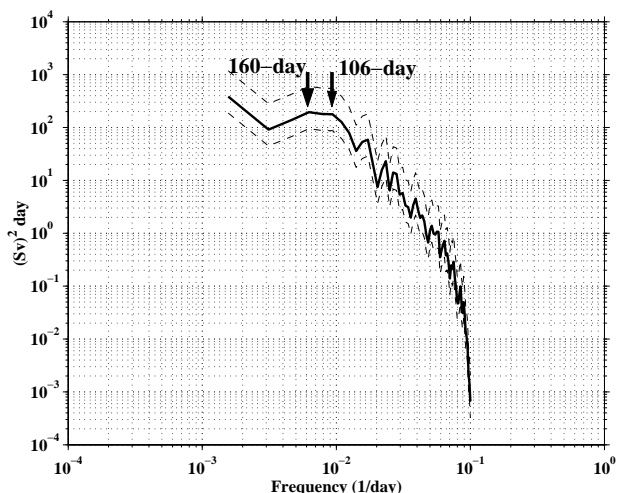


Fig. 5. Power spectral density of the NVT. The thin broken lines indicate the 95% confidence limit. Two arrows show the pronounced peak of the period from 106 to 160 days.

ber to November 1996, September to November 1999 and April to June 2001. During these four events, the NVT first decreased to the minimum value toward the southwest, and then increased to a maximum toward the northeast. In order to identify the distributions of the sea surface height during these four events, the SSHA distributions when the NVT took the minimum and maximum values are shown in Fig. 6. When the NVT took the minimum value at each event, the western part of a cyclonic eddy extended to the observation line, making the NVT southwestward. By contrast, when the NVT took the maximum value, an anticyclonic eddy intruded the observation line. For example, a cyclonic eddy was located in the east side of the observation line in late September 1996. It then moved to the west side of the observation line on November of 1996, while an anticyclonic eddy existed on the west side of the observation line. This eddy pair caused the NVT to reach the maximum value in the 9 years.

In order to illustrate the general relationship between the NVT and mesoscale eddies, we examined the cross-correlation between the NVT and the offshore SSHA. Figure 7 shows the spatial distribution of cross-correlation with different temporal lags from –40 days to 60 days with a 20-day interval. A positive correlation coefficient area appeared around 24–26°N, 130–132°E (Fig. 7(a)). This area then propagated westward close to Okinawa, and the correlation coefficients increased (Fig. 7(b) to (c)). A high positive correlation coefficient area arrived at the east side of the observation line. The diameter of this eddy-type pattern (correlation coefficient > 0.4) is about 300 km (Fig. 7(c)), and its west side occupied the obser-

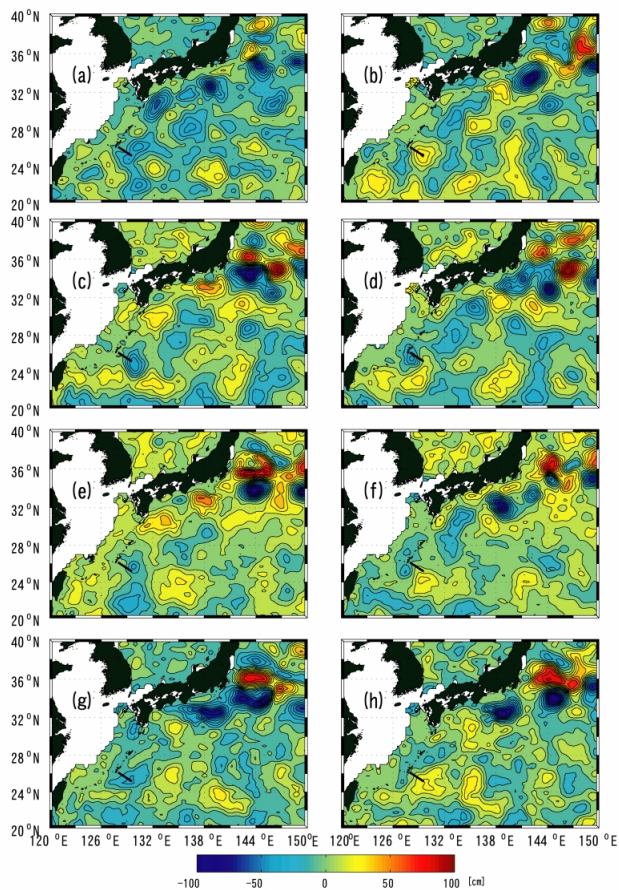


Fig. 6. SSHA distribution when the NVT takes the minimum value and the maximum volume transports in 4 May 1995 (a), 3 July 1995 (b), 30 September 1996 (c), 19 November 1996 (d), 16 September 1999 (e), 15 November 1999 (f), 4 April 2001 (g) and 2 June 2001 (h). The solid line locales southeast of Okinawa in each panel indicates the ocean observation line where the NVT was examined. Contour interval is 10 cm.

vational line, i.e., if it is an anticyclonic (cyclonic) eddy, it could increase (decrease) the NVT across the observational line. Twenty days later, the high positive correlation coefficient area moved to the center of the observation line (Fig. 7(d)) and entered the East China Sea (Fig. 7(e)). Sixty days later, this positive correlation coefficient area extended into the Tokara Strait (Fig. 7(f)) and influenced the Kuroshio, as also pointed out by Ichikawa (2001).

#### 4.2 Interannual variability

In order to examine the long-term variations of the NVT, a 10-month low pass filter was applied to remove the eddy component. The eddy-removed NVT (Fig. 8) showed that the NVT peaks exceed the 95% confidence

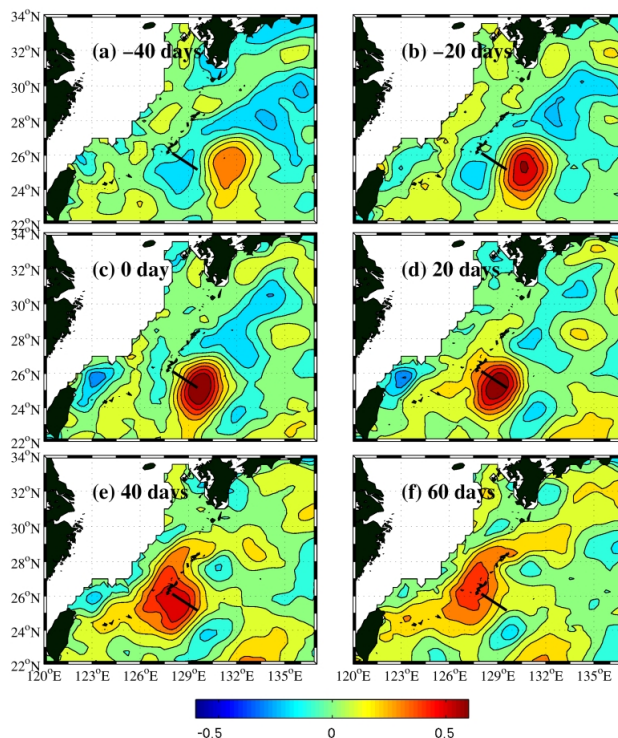


Fig. 7. Spatial distribution of the correlation coefficients between the NVT and the SSHA with different temporal lags: 40 days before (a), 20 days before (b), same time (c), 20 days after (d), 40 days after (e) and 60 days after (f). The solid line locales southeast of Okinawa in each panel indicates the ocean observation line where the volume transport was examined. Contour interval is 0.1.

interval of 2.1 Sv (see Appendix 3 for detail) in the years 1993, 1995, 1997, 1998, 1999 and 2001. These peaks suggest a quasi-biennial oscillation, in which the NVT is larger in the odd years (thick line with arrow in Fig. 8), and smaller in even years, except 1998 (broken line with arrow in Fig. 8).

#### 5. Discussion and Summary

The nine-year-long NVT showed quite a large variation, ranging from  $-10.5$  Sv to  $30.0$  Sv, but the mean NVT is small at  $4.5$  Sv. The mean NVT is very small compared to the mean Kuroshio volume transport of  $43$  Sv in south of Shikoku, Japan across the ASUKA line (Imawaki *et al.*, 2001), and the Kuroshio transport of  $23$  Sv in the East China Sea (Ichikawa and Beardsley, 1993), but its variation is of the same order as the Kuroshio volume transport.

In order to examine the relationship between the NVT and the Kuroshio volume transport, we calculated the coherence and phase between the NVT and the Kuroshio

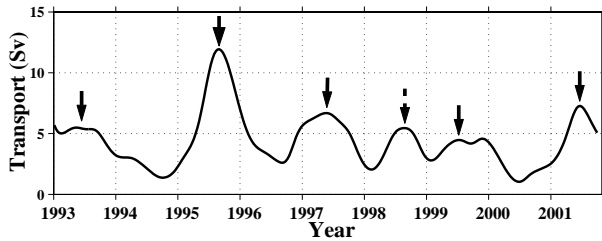


Fig. 8. Time series of 10-month low-pass filtered NVT. Arrows show the transport peaks in individual years. Tick marks along the bottom of time axes indicate the beginning of a year.

volume transport south of Shikoku, Japan across the ASUKA line and the surface Kuroshio Volume Transport (KVT) index in the Tokara Strait (Ichikawa, 2001) (Fig. 9). A coherence peak exceeding the 95% confidence limits appeared around the period of 128 days for the KVT, but no significant peaks were found in the Kuroshio volume transport in the ASUKA line. The phase lag at the peak position of coherence is 179 degrees (64 days). Compared with Fig. 7, it is clear that the NVT is related with the KVT by the mesoscale eddies propagating through the East China Sea, as also pointed by Ichikawa (2001). This also suggests that the mean component of the current flows northeastward as part of Ryukyu Current System, which joins with the northeastward current southeast of Amami-Oshima (Ichikawa *et al.*, 2004). There is no evidence that the NVT directly influences the Kuroshio volume transport south of Shikoku (Fig. 9). Two reasons can be considered for this: 1) it takes more than 60 days for the eddy propagating from the southeast of Okinawa to the southeast of Kyushu through the East China Sea, but less than 1 month for the northeastward current flows northeastward to the southeast of Kyushu along the western side of Ryukyu Islands (suppose the mean current velocity is 20 cm/s). These will decrease the effect of NVT on the Kuroshio volume transport in AUSKA line. 2) The mean of NVT and its variation ( $4.5 \pm 5.5$  Sv) is too small compared with that of the Kuroshio volume transport ( $43 \pm 16$  Sv) in south of Shikoku (here we have converted the Kuroshio volume transport in AUSKA line and its variation from 30-day mean ( $43 \pm 9$  Sv) to 10-day mean ( $43 \pm 16$  Sv)).

In the 10-month low pass filtered NVT data, we found that a quasi-biennial oscillation exists in this region, which is usually believed to be caused by the variation of the Sverdrup transport due to the large-scale wind variation originally resulting from the stratospheric quasi-biennial oscillation (Huesmann and Hitchman, 2001). During the 9 years, the eddy-removed NVT shows a maximum value of 12 Sv in the autumn of 1995. This result is the same as that reported by Liu *et al.* (2000), where they compared

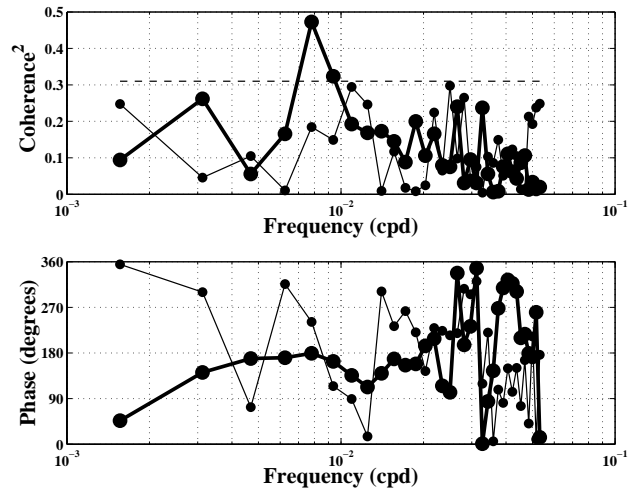


Fig. 9. Coherence between the NVT in the southeast of Okinawa and the Kuroshio transport in the south of Shikoku, Japan across the ASUKA line (thin lines with dots) and the Kuroshio volume transport Index in Tokara strait (solid lines with dots). Upper panel: Coherence squared. Bottom panel: phase lag. The 95% confidence limits are indicated on the figure of coherence with the horizontal broken line.

the averaged volume transport obtained from four cruises every year from 1993 to 1996, and pointed out that the year 1995 is an anomalous year for the current southeast of Okinawa Island, maybe due to the abnormal state of the North Western Pacific Subtropical Gyre associated with the El Niño phenomenon, which occurred from October 1994 to March 1995.

In this paper, the long-term time series of the NVT was estimated based on the ocean observation data of PIES and MADCP using the GEM method. The GEM could not represent the subsurface velocity core in this region (Zhu *et al.*, 2003). In the GEM method, the basic field of the specific volume anomaly is reconstructed by spline interpolating and smoothing the historical hydrographic data in the acoustic travel time coordinate (streamfunction coordinate) under the assumption that the specific volume anomaly profiles have only one vertical mode corresponding to the same acoustic travel time. The subsurface current velocity core structure may be filtered out in the GEM field due to the interpolating and smoothing effect. However, because the NVT error of 5.9 Sv estimated in Appendix 2 already includes the above effect, this does not influence the main result of this paper.

In this paper we have found a close correlation between the volume transport and the sea surface height anomaly difference across the observational line to the southeast of Okinawa Island. Using this relationship, we have derived the nine-year-long record of the NVT from 1992 to 2001, which is the first long-term record of the

northeastward transport with 10-day interval in this area. Our results can be summarized as follows:

(1) The nine-year-long record of the NVT showed that the transport is strongly influenced by eddies, having quite large variations ranging from  $-10.0$  to  $30$  Sv. The nine-year mean NVT and its standard deviation are estimated as  $4.5 \pm 5.5$  Sv toward the northeast.

(2) The large variations of the NVT have a pronounced period around 106 to 160 days, and are accompanied by the mesoscale eddies come from the east. These mesoscale eddies entered the East China Sea, and propagated northward, to influence the Kuroshio volume transport in the Tokara Strait about 60 days later. There is no evidence that the NVT directly influences the Kuroshio volume transport across the ASUKA line in south of Shikoku, Japan.

(3) The 10-month low-pass-filtered NVT data show that the eddy-removed transport varied from 2 to 12 Sv, having a quasi-biennial oscillation.

The present study provides a practical method for continuous long-term monitoring of the transport using satellite altimeter data and coastal tide gauge data in the region southeast of Okinawa Island.

### Acknowledgements

The ocean mooring data used in this paper were obtained by the Japanese Coastal Predictability Experiment Group (J-COPE), from the Frontier Observational Research System for Global Change (FORSGC). We greatly thank Drs. A. Ostrovskii, A. Kaneko, J.-H. Park, I.-S. Han, N. Gohda and S. Umatani for their support in the ship-board work. We also thank the J-COPE/FORSGC members for their helpful comments on the manuscript. Data on the Kuroshio volume transport in the south of Shikoku, Japan was kindly provided by Prof. S. Imawaki of Kyushu University and Dr. H. Uchida of JAMSTEC. The satellite altimeter data and the tide gauge data were provided by the Physical Oceanography Distributed Active Archive Center at the Jet Propulsion Laboratory, AVISO (Archiving Validation and Interpretation of Satellites Oceanographic data), the European Space Agency and the Geographical Survey Institute, Ministry of Land, Infrastructure and Transport Government of Japan, respectively. Finally, two anonymous reviewers are acknowledged for their critical comments on the manuscript and valuable suggestions.

### Appendix 1

Near-surface waters are subject to seasonally-varying heat fluxes, which introduce a corresponding variability of the sea surface height. This appendix explains the detailed method for removing the seasonal signal in the sea surface height for the T/P SSHA data and the tide level data in this paper.

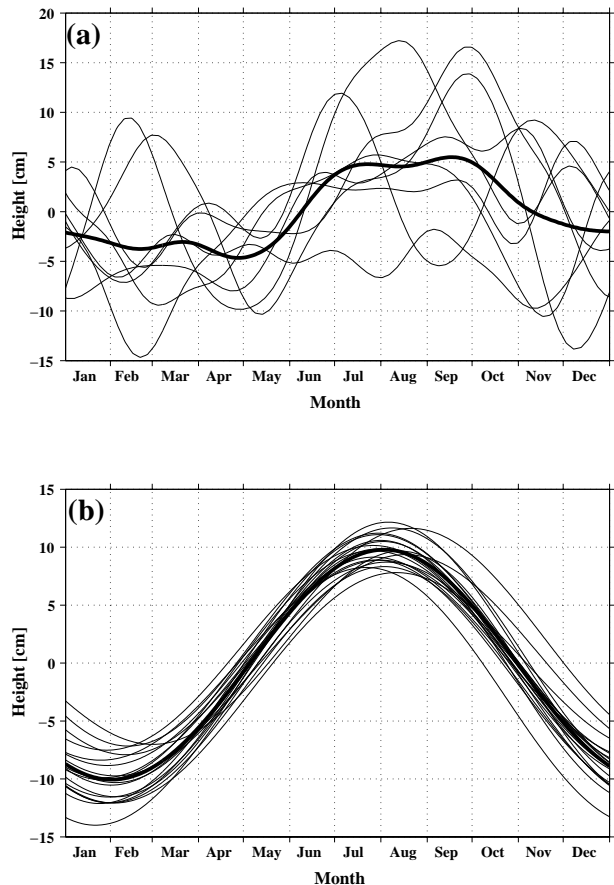


Fig. A1. Upper panel (a): Annual plot of 1-month low pass filtered SSHA. Thin lines and solid line indicate the each of individual SSHA and 8-year averaged SSHA, respectively. Bottom panel (b): Annual plot of 10-month low pass filtered SL. Thin lines and solid line indicate the each of individual SSHA and 21-year averaged SL, respectively.

The SSHA data in the region southeast of Okinawa fluctuate largely due to the approach of mesoscale eddy. It is important to remove the eddy effect, because the SSHA can change about  $\pm 40$  cm when an eddy arrives (Zhu *et al.*, 2002). The SSHA grid data in a zonal box ( $127.5$ – $180^\circ\text{E}$ ,  $24.0$ – $26.0^\circ\text{N}$ ) are averaged to removed the eddy effect in the spatial coordinate. Figure A1(a) shows the annual plot of the eddy-removed SSHA from 1993 to 2000. The 8-year mean SSHA (solid line in Fig. A1(a)) shows a seasonal cycle such that the SSHA is lowest in March and highest in September. The SSHA data are subtracted from this corresponding annual mean SSHA to remove the seasonal signal.

The tide level (SL) data from 1980 to 2000 was first passed by the tide-killer filter to remove the tide, then a 10-month low-pass filter was used to remove long term variations such as mesoscale eddy. Figure A1(b) shows



the annual plot of the eddy-removed SL from 1980 to 2000. The 21-year mean SL (solid line in Fig. A1(b)) shows a seasonal cycle that the SL is lowest in February and highest in August. The SL time series data are processed to remove the seasonal signal using the same method as for the SSHA data.

## Appendix 2

This appendix describes the details of error estimation during the volume transport calculations combined with use of the ocean mooring data and sea surface height anomaly data. The total error of the estimated NVT derives from three sources, as follows.

The first part of error is divided into the accuracy of the NVT estimated using the PIES data and MADCP data. Vertical profiles of geostrophic velocity ( $V_G$ ) are calculated from specific volume anomaly derived by the GEM method. The errors of  $V_G$  have been estimated to be 8.3 cm s<sup>-1</sup>, 5.3 cm s<sup>-1</sup> and 2.1 cm s<sup>-1</sup> for depth ranges of 0–200 dbar, 201–800 dbar and 801–2000 dbar, respectively (Zhu *et al.*, 2003). The error appearing in the NVT is estimated to be 5.1 Sv by integrating the velocity errors in the different depths along the observation line.

The second part of error is the T/P altimeter measurement error and tide level measurement error and the calculation error for removing the seasonal signal. The measurement error of the T/P altimeter along the track and the error of hourly tide data are 2 cm (Fu *et al.*, 1994) and 0.5 cm, respectively. In the calculations for removing the seasonal signal in the SSHAD, 1 cm error may generate due to the different heat flux in the zonal box (Appendix 1). The total error in the SSHAD is  $\sqrt{2^2/5 + 1^2 + 0.5^2}$  1.4 cm. This error will generate an error of 0.7 Sv in the NVT when using the regression relationship to convert to the NVT.

The third part of the error is caused by using the regression relationship between the volume transport and the SSHAD, which is the rms difference (2.8 Sv) between the scatter points of the observational data and the regression line.

The above three error components could propagate and generate an error of  $\sqrt{(5.1^2 + 0.7^2 + 2.8^2)}$  = 5.9 Sv in the final results through the calculations.

## Appendix 3

This appendix describes the details of confidence interval estimation for the low pass filtered NVT time series.

The rms error of the estimated NVT in the 10-day interval resolution is 5.9 Sv (Appendix 2). The 95% confidence interval range for the low pass filtered data is given by the symmetrical distribution for the standardized normal distribution:

$$\mu = \pm z_{\alpha/2} \frac{\sigma}{\sqrt{N}},$$

where  $N$  is the length of the filter in the number of the data,  $\sigma$  is 5.9 Sv. The appropriate values of  $z$  for the normal distribution are  $z_{\alpha/2} = 1.96$  (Emery and Thomson, 1997). The 95% confidence interval ranges for 10-month low pass filtered NVT are estimated to be  $\pm 5.9 \times 1.96 / \sqrt{30 \times 10 / 10} = 2.1$  Sv.

## References

- Book, J., M. Wimbush, S. Imawaki, H. Ichikawa, H. Uchida and H. Kinoshita (2002): Kuroshio temporal and spatial variations south of Japan, determined from inverted-echosounder measurements. *J. Geophys. Res.*, **107**(C9), 3121, doi:10.1029/2001JC000795.
- Emery, W. J. and R. E. Thomson (1997): *Data Analysis Methods in Physical Oceanography*. 1st ed., Elsevier, New York, 634 pp.
- Fu, L.-L., E. J. Christensen, C. A. Yamarone, M. Lefebvre, Y. Menard, M. Dorrer and P. Escudier (1994): TOPEX/POSEIDON mission overview. *J. Geophys. Res.*, **99**(C12), 24369–24381.
- Hanawa, K. and H. Mitsudera (1985): On the data processing of daily mean values of oceanographically data—Note on daily mean sea-level data—. *Bull. Coast. Oceanogr.*, **23**, 79–87 (in Japanese).
- Huesmann, A. S. and M. H. Hitchman (2001): The stratospheric quasi-biennial oscillation in the NECP reanalyses: Climatological structures. *J. Geophys. Res.*, **106**(D11), 11859–11874.
- Ichikawa, H. and R. C. Beardsley (1993): Temporal and spatial variability of volume transport of the Kuroshio in the East China Sea. *Deep-Sea Res.*, **40**, 583–605.
- Ichikawa, H., H. Nakamura, A. Nishina and M. Higashi (2004): Variability of northeastward current southeast of northern Ryukyu Islands. *J. Oceanogr.*, **60**, 351–363.
- Ichikawa, K. (2001): Variation of the Kuroshio in the Tokara Strait induced by meso-scale eddies. *J. Oceanogr.*, **57**, 55–68.
- Imawaki, S., H. Uchida, H. Ichikawa, M. Fukazawa, S. Umatani and the ASUKA Group (2001): Satellite altimeter monitoring the Kuroshio transport south of Japan. *Geophys. Res. Lett.*, **28**(1), 17–20.
- Johns, W. E., T. N. Lee, D. Zhang and R. Zantopp (2001): The Kuroshio East of Taiwan: Moored transport observations from the WOCE PCM-1 Array. *J. Phys. Oceanogr.*, **31**, 1031–1053.
- Lee, T. N., W. E. Johns, C. T. Liu, D. Zhang, R. Zantopp and Y. Yang (2001): Mean transport and seasonal cycle of the Kuroshio east of Taiwan with comparison to the Florida Current. *J. Geophys. Res.*, **106**, 22143–22158.
- Liu, Y. G. and Y. C. Yuan (2000): Variation of the currents east of Ryukyu Islands in 1998. *La mer*, **38**, 179–184.
- Liu, Y. G., Y. C. Yuan, T. Shiga, H. Yamamoto, S. Tsubaki and M. Imai (2000): Circulation southeast of the Ryukyu Islands. p. 23–37. In *Proceedings of China and Japan Joint*

- Symposium on Cooperative Study of Subtropical Circulation System*, China Ocean Press, Beijing.
- Nakano, T., T. Kuragano and Y. Liu (1998): Variations of oceanic conditions east of the Ryukyu Islands. p. 129–140. In *Proceedings of Japan and China Joint Symposium on Cooperative Study of Subtropical Circulation System, 1–4 December 1997, Nagasaki, Japan*, Seikai National Fisheries Research Institute, Nagasaki.
- Shiga, T., D. Ueno, Y. Takatsuki and Y. Liu (2000): Variations of oceanic conditions east of the Ryukyu Islands in 1997. p. 57–65. In *Proceedings of Japan and China Joint Symposium on Cooperative Study of Subtropical Circulation System*, China Ocean Press, Beijing.
- Uchida, H., S. Imawaki and J.-H. Hu (1998): Comparison of Kuroshio Surface velocity derived from satellite altimeter and drifting buoy data. *J. Oceanogr.*, **54**, 115–122.
- Watts, D. R., C. Sun and S. Rintoul (2001): Two-dimensional gravest empirical modes determined from hydrographic observations in the Subantarctic Front. *J. Phys. Oceanogr.*, **31**, 2186–2209.
- Worthington, V. L. and H. Kawai (1972): Comparison between deep sections across the Kuroshio and the Florida Current and Gulf Stream. p. 371–385. In *Kuroshio, Its Physical Aspects*, ed. by H. Stommel and K. Yoshida, Washington Univ. Press.
- Yang, Y., C.-T. Liu, J.-H. Hu and M. Koga (1999): Taiwan Current (Kuroshio) and impinging eddies. *J. Oceanogr.*, **55**, 609–617.
- Yuan, Y., K. Takano, Z. Pan, J. Su, K. Kawatate, S. Imawaki, H. Yu, H. Chen, H. Ichikawa and S. Umatani (1994): The Kuroshio east in the East China Sea and the currents east of Ryukyu Islands during autumn 1991. *La mer*, **32**, 235–244.
- Zhu, X. H., I.-S. Han, J.-H. Park, H. Ichikawa, A. Kaneko, A. Ostrovskii, N. Gohda and S. Umatani (2002): Observation of current and eddy activity east of Okinawa Island. In *Proc. 6th Pacific Ocean Remote Sensing Conference, 2002*, Vol. I, 11–15.
- Zhu, X. H., I.-S. Han, J.-H. Park, H. Ichikawa, K. Murakami, A. Kaneko and A. Ostrovskii (2003): The northeastward current southeast of Okinawa Island observed during November 2000 to August 2001. *Geophys. Res. Lett.*, **30**(2), 1071, doi:10.1029/2002GL015867.